JOURNAL OF MATERIALS SCIENCE 32 (1997) 4803–4806

Agglomeration parameter, aggregation number, and aggregate porosity

HYO-SOON SHIN, BYUNG-KYO LEE
Department of Inorganic Materials Engineering, Kyungpook National University, Taegu, 702-701, Korea

Most ceramic powders contain amounts of agglomerates. Hard agglomerates (aggregates) which do not break up during processing may retard compaction leading to a nonuniform pore–size distribution and/or the formation of internal cracks which act as strength–limiting flaws in the sintered product [1]. So far, however, there have been few reports on the quantitative estimation of aggregation. In this study, the aggregation number is correlated with the agglomeration parameter (A) by a simple model relating aggregate density to compact density. The experiments entailed determining the green densities of seeded pellets. Aggregate density was derived from the relation between the porosities and amounts of added seed. The models and experiments permit quantitative investigation of aggregation in ceramic powders.

1. Introduction

The aggregation of small particles to form extended structures is quite common and has important implications in ceramic processing. It is an essential part of processes such as sol–gel, but can be a major impediment to achieving high densities during uniform compaction [2]. Powder packing in ceramic processing is very important since it greatly influences the properties of the sintered ceramic product [3].

Agglomerates usually take two forms. The first form is often produced during powder manufacture. Crystallites produced during decomposition and subsequent calcination sinter together partially to form a hard agglomerate (aggregate) that requires attrition to disintegrate. The second one is the soft form, and can easily be broken apart with surfactants (and/or slight mechanical action). Particles in soft agglomerates are held together with either van der Waals forces or the surface tension of a liquid phase. In packing ceramic powders soft agglomerates are easily crushed and fill the interparticle pores, but hard agglomerates do not. Therefore, it is important to evaluate the hard agglomerates [4, 5].

Several extensive studies on aggregates have been carried out to date. For example, Brewer *et al.* [6] demonstrated that aggregates of barium titanate and manganese zinc ferrite formed with polyvinyl alcohol. Lange and Metcal [7] observed that aggregates were related to fracture origins, due to differences in green density. Dynys and Halloran [8] investigated aggregated alumina powders and showed that the presence of aggregate retarded the compaction at all stages in the process. In their experiments, however, the degree of aggregation was not evaluated. Berrin *et al.* [9] determined the Hausner and compaction ratios in alumina powders. These are attempts to evaluate agglomeration.

Powder packing is important in the compaction process and it is well known that aggregation can strongly influence the uniformity of powder packing. The theory of packing was derived usually by packing of spheres. Scott [10] showed that for monosized spheres, the random packing co-ordination number was about 8, and the relative density was 64%. Westman and Hugill [11] studied packing of mixtures with particles of two or three different sizes and obtained models showing pore volume versus particle diameter. In spite of these studies on packing, studies showing the role of aggregation in packing have not been carried out.

In this study, we experimentally investigate aggregation and its impact on compaction and density. Aggregate Mn–Zn ferrite powders were synthesized by the alcoholic dehydration method. The aggregation density was obtained from seeded pellets and the agglomeration parameter was derived from the green density. Finally, the aggregation number was related to the agglomeration parameter.

2. Theory

Balek [12] defined an agglomeration parameter, A, in order to evaluate the degree of agglomeration as follows:

$$A = \frac{D}{d} \tag{1}$$

where D and d are median particle diameter determined by sedimentation (agglomerated diameter) and mean diameter by the BET (Brunauer, Emmet and Teller) method (primary particle diameter), respectively [13]. The agglomeration parameter A was the first attempt to evaluate agglomeration, but has not been developed further.

0022–2461

On the other hand, powder densities were measured using a pychnometer and were consistent with true densities. Pores in aggregates could not easily be infiltrated, despite the generally low pressure and densities of aggregates are usually small. Therefore, compacts containing such aggregates decrease in density. Fig. 1 shows a schematic of aggregates in water, for which the powder density is measured. Spherical shapes of powders and aggregates were assumed in calculating the powder density,

$$\rho_t = \frac{m}{\frac{4}{3}\pi\gamma^3}: \quad \text{density of primary particle}$$

and

$$\rho = \frac{Nm}{\frac{4}{3}\pi R^3}: \quad \text{density of aggregate containing } N \text{ primary particles}$$

where ρ_t and ρ are the true and the aggregate density, m is the mean mass of the primary particle, r and R are the mean radii of the primary particle and aggregates, and N is the aggregation number. If it is assumed that only aggregates exist, then from Equation 1 the agglomeration parameter is

$$A^3 = \frac{R^3}{r^3} = \frac{N\rho_t}{\rho} \tag{2}$$

with the shape factor of particles introduced Equation 2 becomes

$$A^3 = \frac{SN\rho_t}{\rho} \tag{3}$$

where S is the ratio of shape factors between the primary particle and aggregate. When the shapes of primary particle and aggregate are spherical, S equals 1. Ring [14] described the growth of the aggregates by a random attachment of particles in Brownian motion; ceramic powder compacts also appear to be a fractal structure. If the aggregate structure is fractal and the aggregate has self-similarity, then the shape of aggregates will also be spherical, and the shape factor $S = 1$. When the primary particle size is very small, the particle shape is generally spherical.

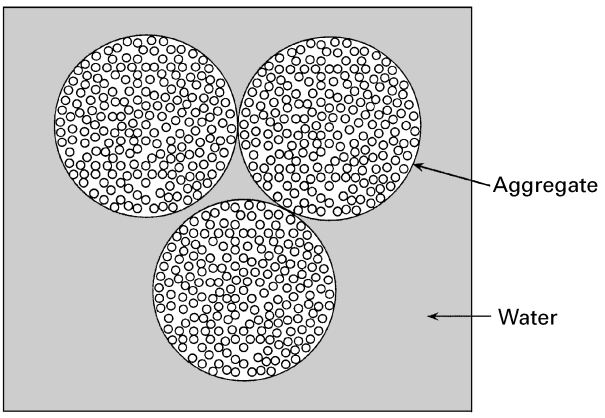

Figure 1 Model of aggregates in water.

The agglomerate density, ρ, can also be defined as:

$$\rho = \frac{m_s + m_p}{V_s + V_p}$$

where m_s and m_p are the masses of the particles and pores and V_s and V_p are the volumes of particles and pores in an aggregate. The true density, ρ_t, is defined as m_s/V_s. Since m_p is negligible compared with m_s, the aggregate density, ρ, becomes

$$\rho = \frac{m_s}{V_s + V_p} = \frac{\rho_t V_s}{V_s + V_p}$$

or

$$\frac{\rho}{\rho_t} = \frac{V_s}{V_s + V_p} \tag{4}$$

Introducing Equation 4 into Equation 3 yields

$$A^3 = SN\left(\frac{V_s + V_p}{V_s}\right) \tag{5}$$

and for $S = 1$, Equation 5 becomes

$$A^3 = N\left(1 + \frac{V_p}{V_s}\right) \tag{6}$$

For aggregates, Equation 6 should be modified, because V_p and V_s can not be measured directly.

V_p can be rewritten as $\varepsilon_a V$ where ε_a is the fractional aggregate porosity, and the total volume V is $V_s + V_p$ then

$$V_p = \varepsilon_a (V_s + V_p) \tag{7}$$

$$\frac{V_p}{V_s} = \frac{\varepsilon_a}{1 - \varepsilon_a} \tag{8}$$

Therefore,

$$A^3 = N\left(1 + \frac{\varepsilon_a}{1 - \varepsilon_a}\right) \tag{9}$$

If the fractional aggregate porosity is known, N may be related to A as

$$A^3 = N(1 + K) \tag{10}$$

where

$$K = \frac{\varepsilon_a}{1 - \varepsilon_a}$$

and K is the constant determined by the aggregate porosity. In powder syntheses using the solution techniques, aggregation mechanisms are assumed to be the same, and the aggregate porosity, ε_a, becomes constant. For example, Scott [10] showed that equi-sized spheres can be packed in spherical containers with a packing ratio of 0.63. From this, 0.37 can be taken as the aggregate porosity and

$$A^3 = N(1 + 0.5873)$$

In general, aggregate porosity is different for random packing due to the different mechanism of aggregation. Therefore, the random packing case can not be explained with the above mentioned model.

3. Experimental procedure

In this study, Mn–Zn ferrite powder, synthesized by an alcoholic dehydration method was used to estimate the agglomeration parameter. This method is a solution technique and therefore the primary particle size distribution is narrow, the particle shape is spherical, and the aggregate shape is spherical also [15].

The starting materials were Mn_3O_4, ZnO, and ferric citrate. The powders of each salt were measured, mixed with 60 wt % aqueous citric acid, and heated to obtain a clear solution. In the later experiments, Mn_3O_4 and ZnO were dissolved in 85 wt % formic acid and boiled to achieve a clear solution. Ferric citrate was separately dissolved in deionized water and heated until boiling. Ammonium hydroxide (14.8 N NH_4OH) was added in order to achieve a clear solution.

The as-prepared citrate or formate solutions were sprayed into a 12-fold volume of reagent grade ethyl alcohol. The resultant (Mn–Zn–Fe)–citrate–formate complex salts were washed with ethyl alcohol, filtered, and dried at 110 °C. A two-step calcination process was adopted where, after an initial calcination at 400 °C in air for 4 h for decomposition of citric and formic radicals, a second calcination was carried out at 900 °C for 20 min in N_2 for formation of the ferrite phase

Calcined powders were crushed by ball milling for 20 h; non-ball-milled powders were used as aggregate seeds. Seeds were mixed from 0 to 15 wt %. Mixed powders were formed into pellets at 100, 150, and 200 MPa. Green densities of pellets were measured by a dimensional method. A scanning electron microscope (SEM) was used to study the morphology of the calcined powders and green bodies.

4. Results and discussion

Fig. 2a shows an SEM micrograph of ball-milled powders, and Fig. 2b, shows the spherical aggregates used as seeds. The primary particle size is uniform and has a near spherical morphology, as shown in the figures.

The aggregate surrounded by primary particles is illustrated in Fig. 3. From this model, the aggregate porosity can be induced as

$$\varepsilon = \varkappa_a \varepsilon_a + \varkappa_p \varepsilon_p \tag{11}$$

$$\varkappa_a + \varkappa_p = 1$$

$$\varepsilon = \varkappa_a \varepsilon_a + (1 - \varkappa_a)\varepsilon_p$$

$$\varepsilon = \varkappa_a(\varepsilon_a - \varepsilon_p) + \varepsilon_p \tag{12}$$

where ε is the total porosity of green body, ε_a is the aggregate porosity, ε_p is the porosity between primary particles, and $\varkappa_a$ and $\varkappa_p$ are the fractions of the aggregate and primary particles. When aggregates are among primary particles, there are three types of pores: one in aggregates, another between primary particles, and the third between primary particles and aggregates. In these types, the pore between the primary particles and the aggregates is similar to the inter-primary-particle pore, because the surface of the aggregate appears as the arrangement of the primary particles. Therefore, the pores can now be sorted into

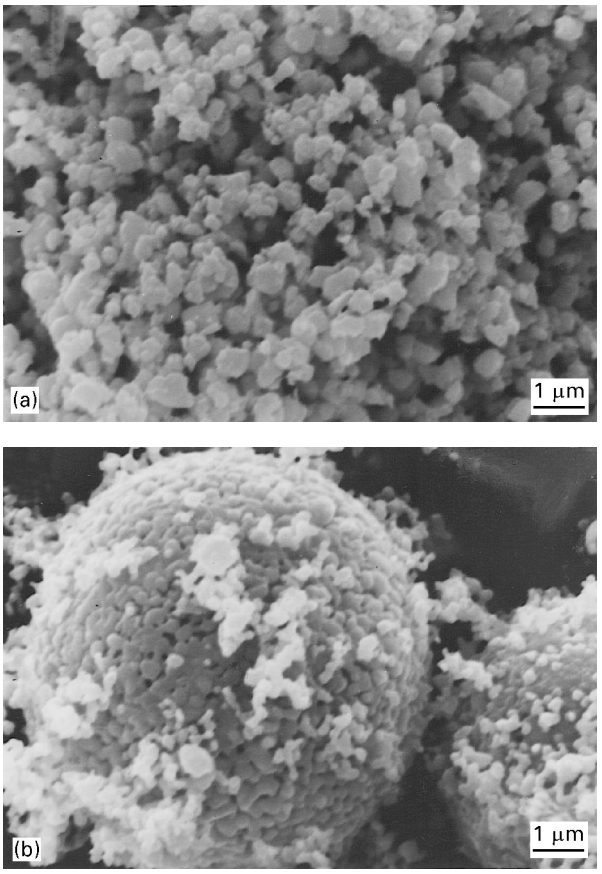

Figure 2 SEM micrographs of (a) reground fine powders and (b) aggregates.

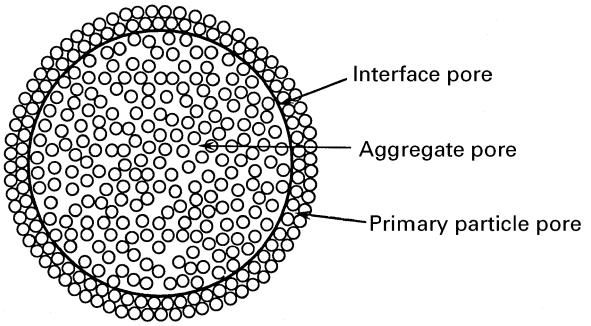

Figure 3 Schematic illustration of three kinds of pores in a green body.

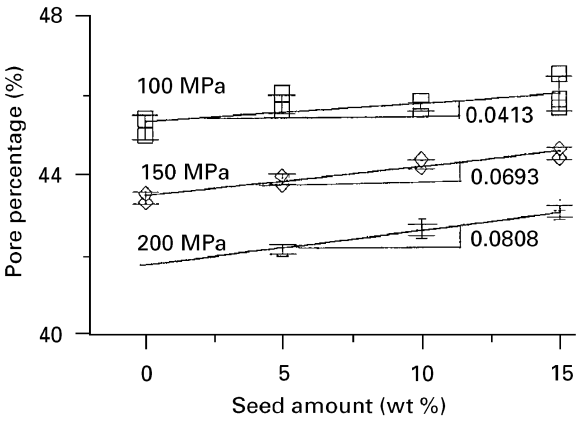

Figure 4 Pore percentage versus seed amount for different pressure values.

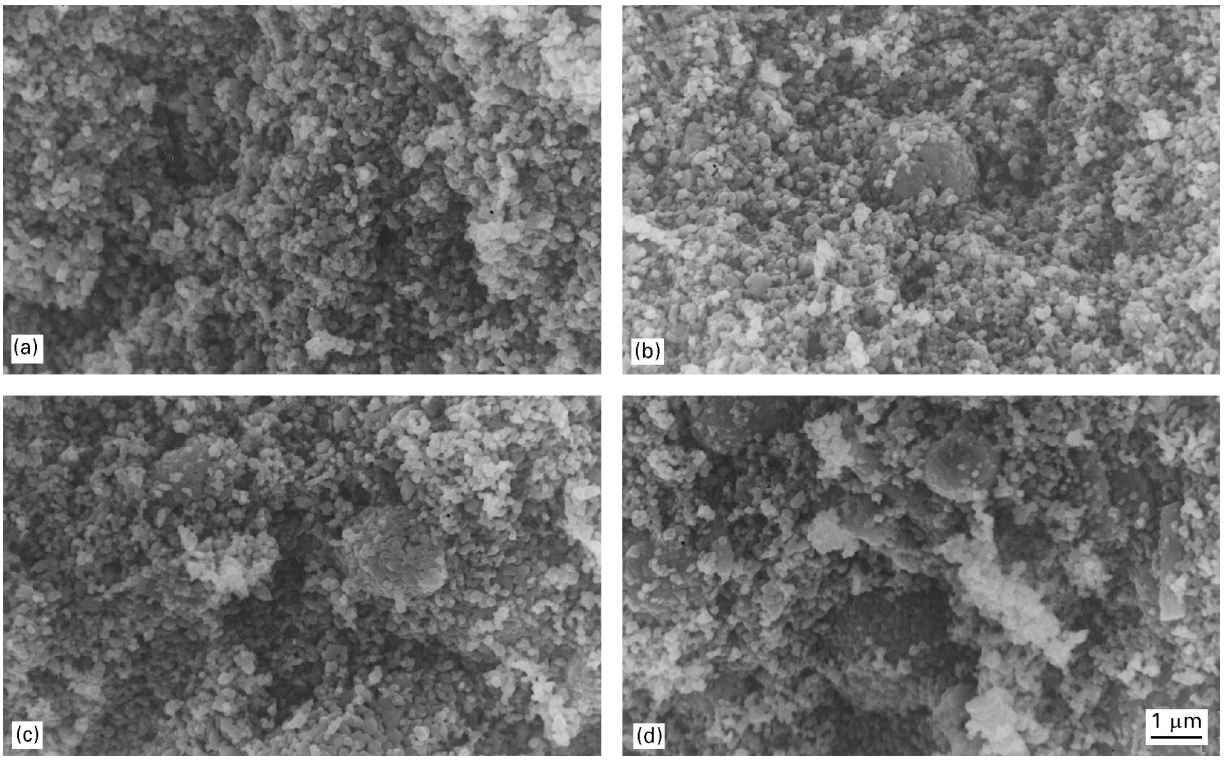

Figure 5 Fracture morphologies of green compacts with variation of seed amounts: (a) 0%, (b) 5%, (c) 10%, and (d) 15%.

two groups, i.e. pores between primary particles and pores in aggregates.

Fig. 4 shows the relation between the seed amounts and the porosity calculated from the green densities (e.g. $1-\rho_t$). Porosities of green bodies increased linearly with the seed amounts. From these data, aggregate porosity, ε_a could be calculated from Equation 12. With the increase of applied pressure from 100 to 150 and 200 MPa, the slopes appear to be 0.0413, 0.0693 and 0.0808, respectively, and the ε_p appear to be 0.4536, 0.4350, and 0.4179, respectively in the figure. Since $\varepsilon_a = \varepsilon_p +$ slope in Equation 12, the ε_a's are calculated to be 0.4949, 0.5043, and 0.4989, respectively. These values are almost the same, and a mean value of 0.4993, can be determined for ε_a.

Fig. 5 shows the aggregates existing in fractured green bodies. When the mixed powders are pressed, aggregates are not crushed. The number of aggregates is increased with increased added seed amounts. In the aggregate, necking between primary particles similarly increases with calcination time, because necking of primary particles is the same in the initial sintering, when shrinkage between particles (pore decreasing) is small [16]. Therefore, aggregate porosity can be determined in the aggregate. If the obtained value of ε_a of 49.93 relative per cent, is introduced into Equation 9, the agglomeration parameter A becomes

$$A^3 = N(1 + 0.9972)$$
$$A^3 \fallingdotseq 2N \quad (13)$$

5. Conclusions

From this study, the conclusions are as follows.

1. From the density, the agglomeration parameter, A, is related to the aggregation number, N, as follows: $A^3 = N(1 + K)$.

2. Green densities were measured with various amounts of added aggregate seeds, and the aggregate porosity, ε_a was found to be 49.93%

3. K was defined from the aggregate porosity and, as a result, the agglomeration parameter, A, can be rewritten as $A^3 \fallingdotseq 2N$.

References

1. M. CIFTCIOGLU, M. AKINC and L. BURKHART, *Amer. Ceram. Soc. Bull.* **65** (1986) 1591.
2. P. MEAKIN, "Better Ceramic Through Chemistry, IV" (Material Research Society, Pittsburgh, 1994) p. 141.
3. J. ZHENG, P. F. JOHNSON and J. S. REED, *J. Amer. Ceram. Soc.* **73** (1990) 1392.
4. F. F. LANGE, "Ceramic Powders" (Elsevier Science Pub. Co., 1983). p. 635.
5. F. F. LANGE, *J. Amer. Ceram. Soc.* **67** (1984) 83.
6. J. A. BREWER, R. H. MOORE and J. S. REED, *ibid.* **60** (1981) 212.
7. F. F. LANGE and M. METCALF, *ibid* **66** (1983) 398.
8. F. W. DYNYS and J. W. HALLORAN, *ibid.* **66** (1983) 655.
9. L. BERRIN, D. W. JOHNSON, JR and D. J. NITTI, *Amer. Ceram. Soc. Bull.* **51** (1972) 840.
10. G. D. SCOTT, *Nature* **188** (1960) 908.
11. A. E. R. WESTMAN and H. R. HUGILL, *J. Amer. Ceram. Soc.* **13** (1930) 767.
12. V. BALEK, *J. Mater. Sci. Lett.* **5** (1970) 714.
13. R. T. TREMPER and R. S. GORDON, "Ceramic Processing before Firing" (Wiley-Interscience, 1978) p. 153.
14. T. A. RING, "Ceramic Powder Processing Science" (Deutsche Keramische Gesellschaft. Co., 1988) p. 681.
15. P. SAINAMTHIP and V. R. W. AMARAKOON, *J. Am. Ceram. Soc.* **71** (1988) C. 92.
16. J. S. REED, "Introduction to the Principles of Ceramic Processing", (Wiley-Interscience, 1988) p. 449.

Received 17 July 1996
and accepted 11 February 1997